ARF suppresses 5'-terminal oligopyrimidine mRNA translation

Kyle A. Cottrell[1], Ryan C. Chiou[1], Jason D. Weber[1,2]

[1]Department of Medicine, Division of Molecular Oncology and [2]Department of Cell Biology and Physiology, Siteman Cancer Center, Washington University School of Medicine, Saint Louis, Missouri, USA

Abstract

Tumor cells require nominal increases in protein synthesis in order to maintain high proliferation rates. As such, tumor cells must acquire enhanced ribosome production. How many of the mutations in tumor cells ultimately achieve this aberrant production is largely unknown. The gene encoding ARF is the most commonly deleted gene in human cancer. ARF plays a significant role in regulating ribosomal RNA synthesis and processing, ribosome export into the cytoplasm, and global protein synthesis. Utilizing ribosome profiling, we show that ARF is a major suppressor of 5'-terminal oligopyrimidine mRNA translation. Genes with increased translational efficiency following loss of ARF include many ribosomal proteins and translation factors. Knockout of *p53* caused a similar increase in 5'-TOP mRNA translation. The 5'-TOP regulators mTORC1, eIF4G1 and LARP1 are dysregulated in ARF and p53 null cells.

Correspondence:
Jason D. Weber, Ph.D.
Department of Medicine
Division of Molecular Oncology
Washington University School of Medicine
660 South Euclid Avenue
Campus Box 8069
St. Louis, MO 63110 USA
Email: jweber@wustl.edu
Telephone: 314-747-3896
Fax: 314-362-0152

32 **Introduction**

33 Accelerated cellular division and macromolecular growth of tumors is dependent on robust protein
34 synthesis. To meet this need, ribosome biogenesis and translation rates are frequently elevated in cancer cells
35 [1]. Increased translation in cancer cells is often driven by activation of the mTORC1 pathway [1].

36 Loss of the gene encoding the ARF tumor suppressor is the most common copy number variation in
37 cancer [2]. ARF is expressed in response to oncogenic stimuli – including the overexpression of Myc, oncogenic
38 Ras and chronic activation of the mTORC1-pathway [3,4]. The canonical function of ARF is to stabilize p53 by
39 sequestering MDM2 in the nucleolus [4-6]. In addition to its canonical role, ARF suppresses global protein
40 synthesis and ribosome biogenesis by regulating rRNA transcription and processing [7-16]. ARF also regulates the
41 translation of specific mRNAs, including VEGFA and DROSHA [10,17].

42 While ARF is known to regulate ribosome biogenesis, the p53-MDM2 axis senses dysregulation of
43 ribosome biogenesis [18]. Free ribosomal proteins, such as RPL11, bind to MDM2 and lead to stabilization of p53
44 [18]. In addition, p53 is known to repress the activity of mTORC1 during times of genotoxic stress [19].

45 The synthesis of ribosomal proteins is tightly regulated by the mTORC1 pathway [20]. Many ribosomal
46 proteins and some translation factors contain a 5'-terminal oligopyrimidine (5'-TOP) motif at the beginning of
47 their mRNAs [21,22]. The translation of 5'-TOP mRNAs is regulated by LARP1 which inhibits translation through
48 disrupting eIF4G1 binding to the 5' end of the mRNA [23-25]. Activation of the mTORC1 pathway leads to
49 inhibition of LARP1 via phosphorylation by AKT and S6-kinase [23]. When phosphorylated, LARP1 binds the
50 3'UTR of 5'-TOP mRNAs and enhances translation [23].

51 Here, we show that ARF selectively regulates the synthesis of ribosomal proteins and translation
52 factors containing 5'-TOP motifs within their mRNAs. Knockdown or knockout of ARF caused increase
53 translation of many 5'-TOP mRNAs. This effect of ARF-loss was dependent on p53 expression. Knockout of *p53*
54 caused a similar increase in the expression of some 5'-TOP mRNA encoded proteins. Finally, we observed
55 dysregulation of many regulators of 5'-TOP mRNA translation.

Results

Increased protein synthesis following loss of ARF

ARF has been previously identified as a regulator of global protein synthesis [10,16]. To confirm these previous findings, we assessed global protein synthesis using wildtype (WT) and *Arf*$^{-/-}$mouse embryonic fibroblasts (MEFs). Polysome profiling of WT and *Arf*$^{-/-}$MEFs revealed a shift of rRNA mass towards polysomes in *Arf*$^{-/-}$, indicating more translation in those cells, Figure 1a. This result is consistent with previous studies [10,16]. We further confirmed this observation by measuring the rate of puromycin incorporation into nascent peptides in WT and *Arf*$^{-/-}$ MEFs. Puromycin is a translation elongation inhibitor that is incorporated into nascent peptide during protein synthesis [26]. Using a puromycin antibody it is possible to detect puromyclylated peptides. We observed an increase in puromycylated proteins in *Arf*$^{-/-}$ MEFs compared to WT MEFs, Figure 1b, further confirming elevated protein synthesis in those cells.

Increased translation efficiency of 5'-TOP mRNAs upon ARF loss

Previously ARF has been identified to not only regulate translation globally but to specifically regulate the translation of a subset of mRNAs [10,17]. To map global translational regulation by ARF we employed ribosome profiling to measure changes in translation efficiency following ARF-loss. We performed ribosome profiling and RNA-seq for WT MEFs transduced with either shSCR or shARF in addition to *Arf*$^{-/-}$ MEFs transduced with shSCR. We identified differentially translated mRNAs using the metric translation efficiency (TE), which is the ratio of ribosome profiling reads to total RNAseq reads for each gene [27]. Most mRNAs show no significant difference in TE upon loss of ARF, Figure 2b and c. However, a subset of mRNAs showed a slight but significant increase in translation following ARF-loss by either knockdown with shARF or knockout of *Arf*. There is a significant correlation between fold change of TE following ARF knockdown and knockout, Figure 2d. Gene ontology analysis of the genes with increased TE following knockout of *Arf* identified multiple GO terms associated with translation, Figure 2e. A closer look at the genes with the biggest increase in TE revealed many ribosomal proteins and translation factors. It has been well established that most ribosomal proteins and

80 many translation factors contain a 5'-TOP motif [21,22]. Analysis of our ribosome profiling results revealed that
81 many of the mRNAs with increased TE are known to contain a 5'-TOP motif, Figure 2f [21]. Furthermore, mRNAs
82 known to contain a 5'-TOP motif show a general increase in TE following knockout of *Arf*, Figure 2g.

83 To validate our ribosome profiling findings, we assessed the mRNA and protein abundance of several
84 5'-TOP genes in MEFs following ARF-loss. By immunoblot we observed increased protein abundance for the 5'-
85 TOP genes PABP, TPT1 and RPL22, Figure 3a-b. The expression of each gene was unchanged at the mRNA level,
86 Figure 3c. Combined with our ribosome profiling results these data support increased translation of 5'-TOP
87 mRNAs in *Arf*-null MEFs. To further validate these findings, we generated a 5'-TOP reporter. The promoter and
88 5'UTR from RPL23A, a 5'-TOP containing gene that showed increased TE upon ARF-loss in our ribosome
89 profiling data, was cloned upstream of firefly luciferase, Figure 3d. This reporter was transfected into WT-
90 shSCR, WT-shARF and *Arf*$^{-/-}$shSCR MEFs along with a plasmid for expression of *Renilla* luciferase as transfection
91 control. We observed increased luciferase activity for our 5'-TOP reporter in ARF-knockdown and knockout
92 MEFs, Figure 3e. This contrasts with a luciferase reporter driven by the SV40 promoter that lacks the 5'-TOP
93 motif. Analysis of the mRNA abundance of the 5'-TOP reporter revealed a slight decrease in mRNA expression
94 in ARF-knockdown and knockout MEFs, Figure 3f. Together these data confirm increased translation efficiency
95 of 5'-TOP containing mRNAs following loss of ARF.

96 **Increased translation efficiency of 5'-TOP mRNAs upon ARF loss is dependent on p53**

97 ARF is a well-known activator of p53 [4,5]. To test whether p53 is required for ARF-dependent regulation
98 of 5'-TOP mRNA translation we performed some of the experiments described above in *p53*$^{-/-}$ MEFs.
99 Knockdown of ARF in *p53*$^{-/-}$ MEFs had no effect on 5'-TOP mRNA protein or mRNA abundance, Figure 4a-b.
100 Furthermore, knockdown of ARF had no effect on the translation of the RPL23A reporter, Figure 4c. There was
101 no difference in polysome abundance between shSCR and shARF transduced *p53*$^{-/-}$ MEFs indicating no changes
102 in total protein synthesis, Figure 4d. However, there were some changes in the abundance 40S and 60S
103 ribosomal subunits based on variations in peak heights. This observation mirrored that seen following

104 knockout of *Arf* in WT MEFs. These findings indicate that p53 is required for ARF-dependent translational
105 regulation of 5'-TOP mRNAs.

106 **Loss of ARF modestly affects the expression or activity of 5'-TOP regulators**

107 The mTOR pathway is known to regulate 5'-TOP mRNAs through the phosphorylation and inactivation
108 of LARP1 [23-25]. LARP1 is phosphorylated by the mTOR and the mTORC1 substrate S6-kinase [23]. Immunoblot
109 analysis of mTORC1 pathway activation in WT and ARF-null MEFs revealed a slight, though inconsistent
110 increase in mTORC1 activity, Figure 4a-b. S6-kinase showed the largest increase, though statistically
111 insignificant, in phosphorylation following ARF-loss, indicating LARP1 maybe phosphorylated and inactivated in
112 those cells. However, inhibition of S6-kinase had no effect on the expression of 5'-TOP encoded proteins,
113 Supplementary Figure 7. Interestingly, we observed a slight increase in mTORC1 pathway activation in *p53*$^{-/-}$
114 MEFs following ARF-knockdown, Supplemental Figure 6. Treatment with the mTOR inhibitor Rapamycin was
115 employed to assess the importance of mTORC1 pathway activity in *Arf*$^{-/-}$ MEFs. Consistent with previous
116 reports, cells treated with rapamycin show reduced mTOR autophosphorylation and reduced expression of the
117 5'-TOP encoded proteins RPL22, PABP and TPT1, Figure 4c-d, [28,29]. These results show that mTORC1 activity is
118 required for maximal expression of 5'-TOP mRNAs in ARF-null MEFs. The slight increase in mTORC1 seen
119 following ARF knockdown or knockout could be driving increased translation of 5'-TOP mRNAs.

120 The 5'-TOP mRNA regulator LARP1 is known to function by competing with the translation initiation
121 factor eIF4G [23,25]. Immunoblot analysis revealed a slight increase in eIF4G expression in ARF-null MEFs, Figure
122 4e-f. The same increase was observed in *p53*$^{-/-}$ MEFs following ARF-knockdown, Supplementary Figure 6. We
123 attempted to overexpress eIF4G1 in WT MEFs via lentiviral transduction, but due to the size of the coding
124 sequence the transduction efficiency was extremely low and thus we were unable to assess the importance of
125 increased eIF4G1 expression in ARF-null MEFs (data not shown).

126 LARP1 is a known regulator of 5'-TOP mRNA translation [23-25]. Immunoblot analysis of WT and ARF-null
127 MEFs showed increase protein abundance for LARP1, Figure 5f. There was no increase in LARP1 mRNA

128 expression in ARF-null MEFs relative to WT MEFs, Figure 5g. Knockdown of ARF in p53$^{-/-}$ MEFs had no effect on
129 LARP1 expression, Supplementary Figure 6. Given the dual role of LARP1 as both an enhancer and repressor of
130 5'-TOP mRNA translation[23] it is possible that elevated expression of LARP1 in this context could drive 5'-TOP
131 mRNA translation. However, knockdown of LARP1 had little to no effect on the expression of several 5'-TOP
132 genes in *Arf*$^{-/-}$ MEFs, Figure 4g-h. Only one of the two shRNAs targeting LARP1 had a significant effect on
133 expression but for only one of the 5'-TOP genes assessed – TPT1. These findings indicate that elevated LARP1
134 expression isn't likely to be the driving force behind increased 5'-TOP mRNA translation in following loss of
135 ARF, though it may have a role in the regulation of specific 5'-TOP mRNAs.

136 **Loss of p53 causes upregulation of 5'-TOP mRNAs**

137 Having observed a role for ARF in regulation 5'-TOP mRNA translation, we next sought to determine if
138 p53, which is tightly coupled to ARF expression, has a similar role. Polysome profiling revealed increased
139 translation in *p53*$^{-/-}$ MEFs, as indicated by higher polysome peaks, Figure 6a. We used immunoblot analysis
140 and qPCR to determine the protein and mRNA expression of some of the 5'-TOP genes studied above. We
141 observed an increase in protein expression for two of the 5'-TOP genes (PABP and TPT1) in the *p53*$^{-/-}$, there
142 was no increase in RNA expression, Figure 6b-d. This is consistent with our findings from ARF-null MEFs.
143 Activity of the RPL23a reporter was significantly increased in *p53*$^{-/-}$ MEFs, though the magnitude was small.
144 However, this experiment is confounded by a decrease in the expression of the SV40 driven reporter. This
145 could arise from a difference in the stability of *Renilla* or firefly luciferase in p53-null vs WT MEFs. Immunoblot
146 analysis of WT and *p53*$^{-/-}$ MEFs revealed an increase in LARP1 expression, like that observed in ARF-null MEFs,
147 Figure 6b and 6e. There was no increase in LARP1 mRNA expression in p53-null MEFs relative to WT MEFs,
148 Figure 6e.

149 **Discussion**

150 Together these data fit well with what is known about the functions of ARF in ribosome biogenesis.
151 ARF is known to repress ribosome biogenesis by affecting rRNA transcription, processing and nuclear export [7-

152 [16]. Changes in 5'-TOP mRNA translation upon ARF-loss would help to balance concomitant changes in rRNA
153 production by providing increases in the necessary ribosome subunit proteins. Increased translation of 5'-TOP
154 mRNAs following loss of the ARF tumor suppressor provides a missing mechanism for the increased rates of
155 translation and ribosome biogenesis seen in many human cancers [30].

156 While many of the functions of ARF in regulating ribosome biogenesis are p53 independent, we show
157 here that the regulation of 5'-TOP mRNAs by ARF requires p53 expression. Furthermore, we show that loss of
158 p53 partially phenocopies the effects of ARF-loss on 5'-TOP mRNA translation. These data suggest that
159 canonical ARF-MDM2-p53 axis plays an important role in 5'-TOP mRNA translation. Interestingly, free
160 ribosomal proteins, such as RPL11, are known to activate p53 through binding MDM2[18]. Elevated expression
161 5'-TOP containing ribosomal proteins following p53-loss would complete a feedback loop.

162 It is unclear what factors drive increased 5'-TOP mRNA translation following loss of ARF. We observed
163 increased expression and activity for several regulators of 5'-TOP mRNA translation. Increased mTORC1
164 activity likely contributes to improved translation efficiency of 5'-TOP mRNAs in ARF-null cells, however the
165 increased mTORC1 activity observed in ARF-null MEFs is very modest. By inhibiting mTOR with rapamycin we
166 showed that maximal expression of 5'-TOP encoded proteins requires mTOR activity. mTORC1 regulates 5'-
167 TOP mRNA translation through phosphorylation and inactivation of LARP1. LARP1 acts to balance 5'-TOP
168 mRNA translation through inhibition of translation when dephosphorylated and enhancing translation when
169 phosphorylated [23]. Dephosphorylated LARP1 binds the 5'-TOP motif and blocks binding of eIF4G1. We
170 observed increased expression of both eIF4G1 and LARP1 following ARF-loss. Because of technical limitations
171 described above it is difficult to assess the role of eIF4G1 via overexpression in this system. In addition,
172 because eIF4G1 is a key component of translation initiation, knockdown of eIF4G1 would likely be cytotoxic or
173 generate many pleiotropic effects making it difficult to evaluate the role of eIF4G1 expression in regulation 5'-
174 TOP mRNA translation following loss of ARF. While we were unable to assess the role of eIF4G1 in this system
175 we did investigate the importance of LARP1 expression. Knockdown of LARP1 in *Arf*$^{-/-}$ MEFs had only modest

176 effects on 5'-TOP mRNA expression, with one shRNA causing a significant reduction in the expression of the 5'-
177 TOP mRNA encoded protein TPT1. This suggests that at least for TPT1, LARP1 may modestly enhance
178 translation. Because phosphorylated LARP1 is known to enhance 5'-TOP mRNA translation this result is
179 consistent with active mTORC1 in *Arf*$^{-/-}$ MEFs. We suspect that increased 5'-TOP mRNA translation in ARF-null
180 MEFs is likely caused not by increased activity or expression of mTORC1, eIF4G1 or LARP1 alone – but instead
181 small changes in activity or expression of each of those factors contributed to increased 5'-TOP mRNA
182 translation.

183 **Materials and Methods**

184 **Cell culture**

185 WT (C57BL/6J), Arf$^{-/-}$ (B6.129X1-*Cdkn2*^{atm1Cjs}/KaiJ), *p53*$^{flox/flox}$ (FVB.129-*Trp53*^{tm1Brn}) mouse embryonic
186 fibroblasts were cultured in Dulbecco's modified Eagle's medium (DMEM) (Hyclone) with 10% fetal bovine
187 serum (Invitrogen), 2 mM glutamine (Hyclone), 0.1 mM nonessential amino acids (Hyclone), 1 mM sodium
188 pyruvate (Hyclone), and 2 µg/ml gentamicin (Invitrogen). Low passage MEFs, between 1-4, were used for all
189 experiments.

190 **Viral Production and Transduction**

191 Lentivirus was produced by Lipofectamine 2000 (Inivitrogen) transfection of 293T cells with pCMV-VSV-
192 G, pCMV-ΔR8.2, and either pLKO.1-puro for shRNAs or pLVX-puro for overexpression. Virus was harvested 48
193 hours post-transfection. Cells were transduced with lentivirus for 16 hours in the presence of 10 µg/mL
194 protamine sulfate. The cells were selected with puromycin at 2 µg/mL for two days. The sequences for the
195 shRNA-scramble (shSCR) and shRNA-ARF (shARF) were described previously [16].

196 **Measurement of Bulk Translation**

197 For polysome profiling, translation was inhibited by the addition of 50 µg/mL cycloheximide for 5
198 minutes at 37 °C in culture media. The cells were then washed with PBS, trypsinized and resuspened in culture
199 media. The cells were pelleted and washed with PBS prior to lysis in polysome lysis buffer (20 mM Tris pH

200 7.26, 130 mM KCl, 10 mM $MgCl_2$, 2.5 mM DTT, 0.5% NP-40, 0.2 mg/mL heparin, 0.5% sodium deoxycholate, 50
201 µg/mL cycloheximide and 200 units/mL RNasin (Invitrogen)). Lysis occurred over 10 minutes on ice prior to
202 clarification at 8,000 g for 10 minutes at 4 °C. The absorbance at 260 nm was determined for each sample and
203 an equal number of absorbance units for each sample was overlaid onto a 10-50% sucrose gradient made with
204 sucrose gradient buffer (10 mM Tris pH 7.26, 60 mM KCl, 10 mM $MgCl_2$, 1 mM DTT, 0.1 mg/mL heparin, 10
205 µg/mL cycloheximide). The gradients were subjected to ultracentrifugation at 36000 rpm for 3 hours at 4 °C. A
206 Teledyne Isco fractionation system with UV detector was used to determine absorbance at 254 nm along the
207 gradient.

208 For measurement of translation rates by puromycin incorporation, MEFs were treated with 10 µM
209 puromycin at room temperature for the times indicated. As a control, cells were also treated with 100 µg/mL
210 cycloheximide for 5 minutes at 37 °C prior to addition of puromycin. Immediately following treatment, the
211 cells were washed with 1x PBS containing 100 µg/mL cycloheximide to inhibit further puromycin labeling. The
212 cells were harvested and lysed in RIPA buffer with 1x HALT (Pierce) and 100 µg/mL cycloheximide.
213 Immunoblot was performed as described above with anti-puromycin antibody (DSHB, University of Iowa).

214 **Plasmid Construction**

215 The 5'-TOP reporter for Rpl23a was made by PCR amplification of a region encompassing 500 bp
216 upstream of the annotated transcription start site to the start codon using primers RPL23A Promoter Forward:
217 5'- GTACCTCGAGGAGCTATAAAGGGAAACCCTGTCTC -3' and RPL23A 5'UTR Reverse: 5'-
218 GTACCCATGGTGCTTGGCTGAAAAGGATGGCCC-3'. The PCR product was digested with XhoI and NcoI and
219 ligated into pGL3-control (Promega). The resulting plasmid, pGL3-RPL23A-FF, was confirmed by Sanger
220 sequencing.

221 To make pGL3-Renilla, Renilla luciferase was PCR amplified from pMT-DEST48-FLP [31] with Renilla
222 Luciferase Forward: 5'-TGGAAGCTTGGCATTCCGGTACTGTTGGTAAAGCCACCATGACTTCGAAAGTTTATG-3' and
223 Renilla Luciferase Reverse: 5'-TGGAAGCTTTTATTATTGTTCATTTTTGAGAAC-3' and digested with HindIII (NEB).

224 Renilla luciferase was then ligated into pGL3-Control digested HindIII (NEB) to make pGL3-Renilla-FF. To
225 remove the firefly luciferase coding sequence, the plasmid was digested with NarI and XbaI (NEB),
226 subsequently the ends were blunted with Klenow (NEB) and the plasmid was ligated. The resulting plasmid
227 pGL3-Renilla-deltaFF was confirmed by Sanger sequencing.

228 **Transfection of MEFs and Luciferase Assay**

229 The day before transfection $1x10^5$ cells were plated per well in a six well dish. The cells were
230 transfected with Fugene6 (Promega) and 1 ug each of either pGL3-control or pGL3-Rpl23a and pGL3-Renilla.
231 After 24 hours the cells were washed briefly with 1x PBS prior to measurement of luciferase activity by Dual
232 Luciferase Reporter Assay (Promega).

233 **Ribosome Profiling and RNAseq**

234 For RNAseq, total RNA was isolated from the appropriate cells using the Direct-zol RNA MiniPrep
235 (Zymo) with Trizol (Invitrogen) for initial cell lysis. Contaminating genomic DNA was removed by treatment
236 with Turbo DNA-free Kit per the manufacturers protocol (Invitrogen). The RNA concentration was determined
237 by Qubit RNA BR Assay (Invitrogen) and ribosomal RNA was removed using the RiboZero Gold rRNA Removal
238 Kit (Illumina) per the manufacturers protocol.

239 The ribo-depleted RNA (10 µL) was then fragmented by adding one volume of 2x Fragmentation Buffer
240 (0.5 M EDTA, 0.1 M Na_2CO_3, 0.1 M $NaHCO_3$) and incubating at 95 °C for 20 minutes. Fragmentation was
241 inhibited by the addition of 280 µL of Stop Solution (3 M NaOAc pH 5.5, 15 mg/mL GlycoBlue (Invitrogen)). The
242 RNA was the precipitated by the addition of ethanol. The RNA was resuspended in 10 mM Tris pH 8.0 and
243 resolved on a 15% acrylamide Urea-TBE gel (Bio-Rad). A region containing fragments between 17-34 nt (the
244 same size as those isolated for ribosome profiling [32]) was excised and extracted overnight in RNA Extraction
245 buffer (0.3 M NaOAc pH 5.5, 1 mM EDTA and 0.25% Sodium dodecylsulfate). The extracted RNA was
246 precipitated by ethanol precipitation and subsequently used for sequencing library preparation as described
247 below.

248 Ribosome footprinting was performed as described previously [32],with the use of RNase T1 (Thermo
249 Scientific) instead of RNase I for the footprinting step, see Supplementary Figure 2. The lysates were treated
250 with 700 units of RNase T1 for 1 hour at room temperature with gentle mixing.

251 Following purification of the RNA footprints, sequencing library production was carried out for both
252 the fragmented total RNA and ribosome footprints using the previously described protocol [32].The RNAseq and
253 ribosome profiling libraries were multiplexed and sequenced on a HiSeq 3000 (Illumina) by the Washington
254 University Genome Technology Access Center.

255 **Data and Code Availability**

256 Raw sequencing reads are available at https://www.ncbi.nlm.nih.gov/geo (XXXXXXXX). Scripts used for
257 analysis of differential expression and TE are available at GitHub (XXXXXXXX).

258 **Analysis of Sequencing Data**

259 The ribosome profiling and RNAseq reads were processed to remove short reads, reads lacking the
260 sequencing adapter and adapter only reads using *fastx_clipper* [33]. Indexes, adapter and other sequences
261 introduced during library production were removed by *umi-tools* [34] and *cutadapt* [35]. Sequencing reads
262 mapping to rRNA or ncRNAs were removed using *Bowtie2* [36]. The processed reads were then aligned to the
263 mouse genome (UCSC, mm10) using *TopHat* [37].Read counts of those aligning to the coding sequence of each
264 gene was then determined by *HTSeq* [38]. Differential translation efficiency was determined using *DESeq2* [39].

265 **Immunoblot**

266 Cell pellets were lysed and sonicated in RIPA Buffer (50 mM Tris pH 7.4, 150 mM NaCl, 1% Triton X-100,
267 0.1% sodium dodecyl sulfate and 0.5% sodium deoxycholate) with 1x HALT Protease Inhibitor (Pierce).
268 Seventy-five micrograms of protein lysate were resolved on 4-12% TGX Acrylamide Stain-Free gels (Bio-Rad).
269 Stain-Free gels were imaged prior to transfer to PVDF membrane (Millipore). The blots were then probed with
270 the appropriate primary antibodies: Primary antibodies: Abcam - PABP (ab21060); Bethyl - GAPDH (A300-
271 641A), LARP1 (A302-087A); Cell Signaling Technologies - TPT1(5128), p-MTOR(2971), p-S6(2215S), p-

272 S6K(9205S), p-4EBP1(2855S), eIF4G1(2858), p53(2524S); Santa Cruz Biotechnology - ARF(sc-32748), RPL22(sc-
273 136413), University of Iowa, DSHB - puromycin. Primary antibodies were detected with horseradish-
274 peroxidase conjugated secondary antibodies (Jackson ImmunoResearch) and detection was carried out with
275 Clarity Western ECL Substrate (Bio-Rad).

276 **Quantitative PCR**

277 Total RNA was isolated using the Nucleospin RNA (Macherey-Nagel) with on column DNase treatment.
278 Reverse transcription to make cDNA was performed with iScript Supermix (Bio-Rad). For qPCR the primers
279 listed in the Supplementary Information were used with iQ Sybr Green (Bio-Rad). Fold change in RNA
280 expression was determined by the ΔΔCt method with normalization to PSMA5, TOMM20 and ATP5B. The
281 normalization genes were chosen based on steady expression across all samples as measured by RNA-seq.

282

283

284 **Acknowledgements**

285 We thank Dr. Len Maggi for preparation of MEFs and guidance. This work was supported by: 5T32HL007088-
286 42 and F32GM131514 to KAC; R01CA190986-03 and DOD W81XWH-15-1-0388 to JDW and the Longer Life
287 Foundation: An RGA/Washington University Partnership.

288

289 **Author Contributions**

290 KAC and JDW conceived the project. KAC performed the experiments and data analysis. RC generated the
291 luciferase reporter constructs. KAC wrote the manuscript. All authors edited the manuscript.

292

293 **Competing interests**

294 The author(s) declare no competing interests.

295

296

297 **References**

298 1 Robichaud, N., Sonenberg, N., Ruggero, D. & Schneider, R. J. Translational Control in Cancer. *Cold Spring Harbor*
299 *Perspectives in Biology* **11** (2019).
300 2 Zack, T. I. *et al.* Pan-cancer patterns of somatic copy number alteration. *Nat Genet* **45**, 1134-1140,
301 doi:10.1038/ng.2760 (2013).
302 3 Miceli, A. P., Saporita, A. J. & Weber, J. D. Hypergrowth mTORC1 signals translationally activate the ARF tumor
303 suppressor checkpoint. *Mol Cell Biol* **32**, 348-364, doi:10.1128/MCB.06030-11 (2012).
304 4 Sherr, C. J. & Weber, J. D. The ARF/p53 pathway. *Curr Opin Genet Dev* **10**, 94-99 (2000).
305 5 Weber, J. D., Taylor, L. J., Roussel, M. F., Sherr, C. J. & Bar-Sagi, D. Nucleolar Arf sequesters Mdm2 and activates
306 p53. *Nat Cell Biol* **1**, 20-26, doi:10.1038/8991 (1999).
307 6 Weber, J. D. *et al.* Cooperative signals governing ARF-mdm2 interaction and nucleolar localization of the
308 complex. *Mol Cell Biol* **20**, 2517-2528 (2000).
309 7 Qi, Y. *et al.* p19ARF directly and differentially controls the functions of c-Myc independently of p53. *Nature* **431**,
310 712-717, doi:10.1038/nature02958 (2004).
311 8 Brady, S. N., Yu, Y., Maggi, L. B. & Weber, J. D. ARF impedes NPM/B23 shuttling in an Mdm2-sensitive tumor
312 suppressor pathway. *Mol Cell Biol* **24**, 9327-9338, doi:10.1128/MCB.24.21.9327-9338.2004 (2004).
313 9 Lessard, F. *et al.* The ARF tumor suppressor controls ribosome biogenesis by regulating the RNA polymerase I
314 transcription factor TTF-I. *Mol Cell* **38**, 539-550, doi:10.1016/j.molcel.2010.03.015 (2010).
315 10 Kuchenreuther, M. J. & Weber, J. D. The ARF tumor-suppressor controls Drosha translation to prevent Ras-
316 driven transformation. *Oncogene* **33**, 300-307, doi:10.1038/onc.2012.601 (2014).
317 11 Eymin, B. *et al.* Human ARF binds E2F1 and inhibits its transcriptional activity. *Oncogene* **20**, 1033-1041,
318 doi:10.1038/sj.onc.1204220 (2001).
319 12 Ayrault, O. *et al.* Human tumor suppressor p14ARF negatively regulates rRNA transcription and inhibits UBF1
320 transcription factor phosphorylation. *Oncogene* **25**, 7577-7586, doi:10.1038/sj.onc.1209743 (2006).
321 13 Dai, M. S. *et al.* Physical and functional interaction between ribosomal protein L11 and the tumor suppressor
322 ARF. *J Biol Chem* **287**, 17120-17129, doi:10.1074/jbc.M111.311902 (2012).
323 14 Bertwistle, D., Sugimoto, M. & Sherr, C. J. Physical and functional interactions of the Arf tumor suppressor
324 protein with nucleophosmin/B23. *Mol Cell Biol* **24**, 985-996 (2004).
325 15 Saporita, A. J. *et al.* RNA helicase DDX5 is a p53-independent target of ARF that participates in ribosome
326 biogenesis. *Cancer Res* **71**, 6708-6717, doi:10.1158/0008-5472.CAN-11-1472 (2011).
327 16 Apicelli, A. J. *et al.* A non-tumor suppressor role for basal p19ARF in maintaining nucleolar structure and
328 function. *Mol Cell Biol* **28**, 1068-1080, doi:10.1128/MCB.00484-07 (2008).
329 17 Kawagishi, H. *et al.* ARF suppresses tumor angiogenesis through translational control of VEGFA mRNA. *Cancer*
330 *Res* **70**, 4749-4758, doi:10.1158/0008-5472.CAN-10-0368 (2010).
331 18 Bursac, S., Brdovcak, M. C., Donati, G. & Volarevic, S. Activation of the tumor suppressor p53 upon impairment
332 of ribosome biogenesis. *Biochim Biophys Acta* **1842**, 817-830, doi:10.1016/j.bbadis.2013.08.014 (2014).
333 19 Hasty, P., Sharp, Z. D., Curiel, T. J. & Campisi, J. mTORC1 and p53: clash of the gods? *Cell Cycle* **12**, 20-25,
334 doi:10.4161/cc.22912 (2013).
335 20 Morita, M. *et al.* mTOR coordinates protein synthesis, mitochondrial activity and proliferation. *Cell Cycle* **14**, 473-
336 480, doi:10.4161/15384101.2014.991572 (2015).
337 21 Yamashita, R. *et al.* Comprehensive detection of human terminal oligo-pyrimidine (TOP) genes and analysis of
338 their characteristics. *Nucleic Acids Research* **36**, 3707-3715, doi:10.1093/nar/gkn248 (2008).
339 22 Levy, S., Avni, D., Hariharan, N., Perry, R. P. & Meyuhas, O. Oligopyrimidine tract at the 5' end of mammalian
340 ribosomal protein mRNAs is required for their translational control. *Proc Natl Acad Sci U S A* **88**, 3319-3323,
341 doi:10.1073/pnas.88.8.3319 (1991).
342 23 Hong, S. *et al.* LARP1 functions as a molecular switch for mTORC1-mediated translation of an essential class of
343 mRNAs. *eLife* **6**, e25237, doi:10.7554/eLife.25237 (2017).
344 24 Tcherkezian, J. *et al.* Proteomic analysis of cap-dependent translation identifies LARP1 as a key regulator of
345 5'TOP mRNA translation. *Genes Dev* **28**, 357-371, doi:10.1101/gad.231407.113 (2014).

346 25 Lahr, R. M. *et al.* La-related protein 1 (LARP1) binds the mRNA cap, blocking eIF4F assembly on TOP mRNAs. *Elife*
347 **6**, doi:10.7554/eLife.24146 (2017).
348 26 NATHANS, D. PUROMYCIN INHIBITION OF PROTEIN SYNTHESIS: INCORPORATION OF PUROMYCIN INTO PEPTIDE
349 CHAINS. *Proc Natl Acad Sci U S A* **51**, 585-592, doi:10.1073/pnas.51.4.585 (1964).
350 27 Ingolia, N. T., Ghaemmaghami, S., Newman, J. R. & Weissman, J. S. Genome-wide analysis in vivo of translation
351 with nucleotide resolution using ribosome profiling. *Science* **324**, 218-223, doi:10.1126/science.1168978 (2009).
352 28 Jefferies, H. B. *et al.* Rapamycin suppresses 5'TOP mRNA translation through inhibition of p70s6k. *EMBO J* **16**,
353 3693-3704, doi:10.1093/emboj/16.12.3693 (1997).
354 29 Tang, H. *et al.* Amino acid-induced translation of TOP mRNAs is fully dependent on phosphatidylinositol 3-
355 kinase-mediated signaling, is partially inhibited by rapamycin, and is independent of S6K1 and rpS6
356 phosphorylation. *Mol Cell Biol* **21**, 8671-8683, doi:10.1128/MCB.21.24.8671-8683.2001 (2001).
357 30 Robichaud, N., Sonenberg, N., Ruggero, D. & Schneider, R. J. Translational Control in Cancer. *Cold Spring Harbor*
358 *Perspectives in Biology* **11**, doi:10.1101/cshperspect.a032896 (2019/07/01).
359 31 Cottrell, K. A., Szczesny, P. & Djuranovic, S. Translation efficiency is a determinant of the magnitude of miRNA-
360 mediated repression. *Sci Rep* **7**, 14884, doi:10.1038/s41598-017-13851-w (2017).
361 32 McGlincy, N. J. & Ingolia, N. T. Transcriptome-wide measurement of translation by ribosome profiling. *Methods*
362 **126**, 112-129, doi:10.1016/j.ymeth.2017.05.028 (2017).
363 33 FASTX-Toolkit (2010).
364 34 Smith, T., Heger, A. & Sudbery, I. UMI-tools: modeling sequencing errors in Unique Molecular Identifiers to
365 improve quantification accuracy. *Genome Res* **27**, 491-499, doi:10.1101/gr.209601.116 (2017).
366 35 Martin, M. Cutadapt removes adapter sequences from high-throughput sequencing reads. *EMBnet.journal* **17**
367 (2011).
368 36 Langmead, B. & Salzberg, S. L. Fast gapped-read alignment with Bowtie 2. *Nat Methods* **9**, 357-359,
369 doi:10.1038/nmeth.1923 (2012).
370 37 Trapnell, C., Pachter, L. & Salzberg, S. L. TopHat: discovering splice junctions with RNA-Seq. *Bioinformatics* **25**,
371 1105-1111, doi:10.1093/bioinformatics/btp120 (2009).
372 38 Anders, S., Pyl, P. T. & Huber, W. HTSeq--a Python framework to work with high-throughput sequencing data.
373 *Bioinformatics* **31**, 166-169, doi:10.1093/bioinformatics/btu638 (2015).
374 39 Love, M. I., Huber, W. & Anders, S. Moderated estimation of fold change and dispersion for RNA-seq data with
375 DESeq2. *Genome Biol* **15**, 550, doi:10.1186/s13059-014-0550-8 (2014).

376

377

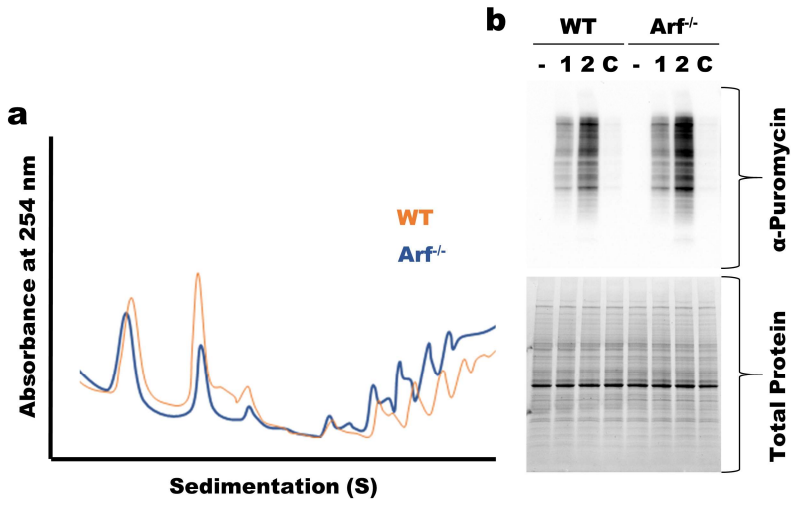

Figure 1: Upregulation of translation following loss of ARF

a Polysome profiling showing increased polysome peaks in *Arf*$^{-/-}$ MEFs **b** Puromycin translation assay showing increased protein production in *Arf*$^{-/-}$ MEFs. – untreated, 1 and 2 treatment with puromycin for 1 or 2 minutes, C indicates cells that were treated with cycloheximide prior to puromycin treatment for 2 minutes.

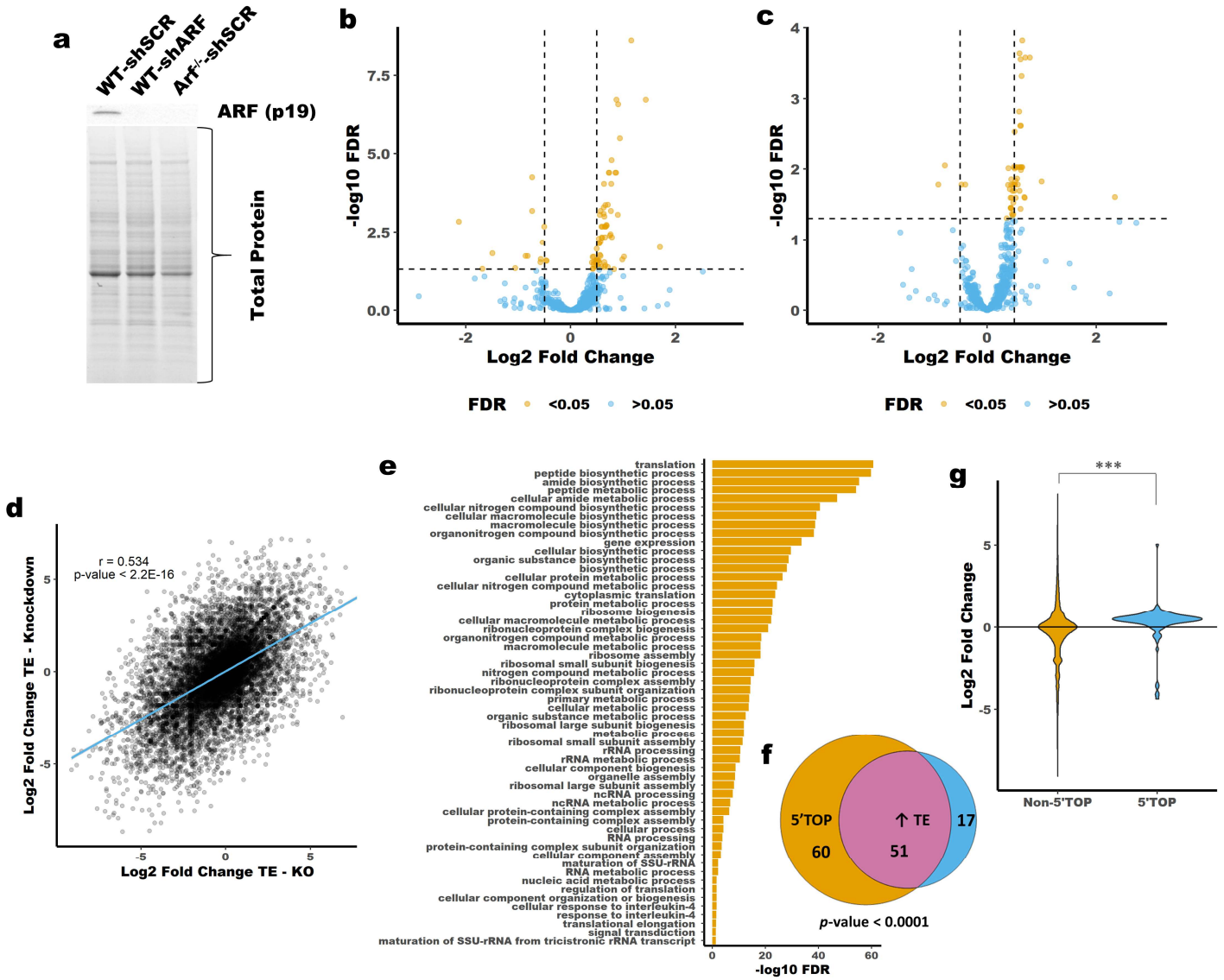

Figure 2: Ribosome profiling reveals upregulation of 5'-TOP mRNA translation following loss of ARF

a Immunoblot showing knockdown and knockout of *Arf* in MEFs. **b** Volcano plot showing Log2 Fold Change of TE between WT-shSCR and *ARF*$^{-/-}$-shSCR MEFs or WT-shSCR and WT-shARF MEFs **c**. Vertical lines are Log2 Fold Change of ±0.5. Horizontal line is FDR corrected *p*-value of 0.05. **d** Correlation between Fold Change of TE following ARF knockout (x-axis) or ARF knockdown (y-axis). **e** Geno ontology terms associated with genes that have increased TE following ARF knockout. **f** Venn-diagram showing overlap between mRNAs with increased TE and the presence of a 5'-TOP motif. **g** Violin plot showing the TE of mRNAs known to contain a 5'-TOP motif versus those that are not known to contain the motif [21]. *** *p*-value <0.00001; chi-squared test (**f**) or t-test (**g**).

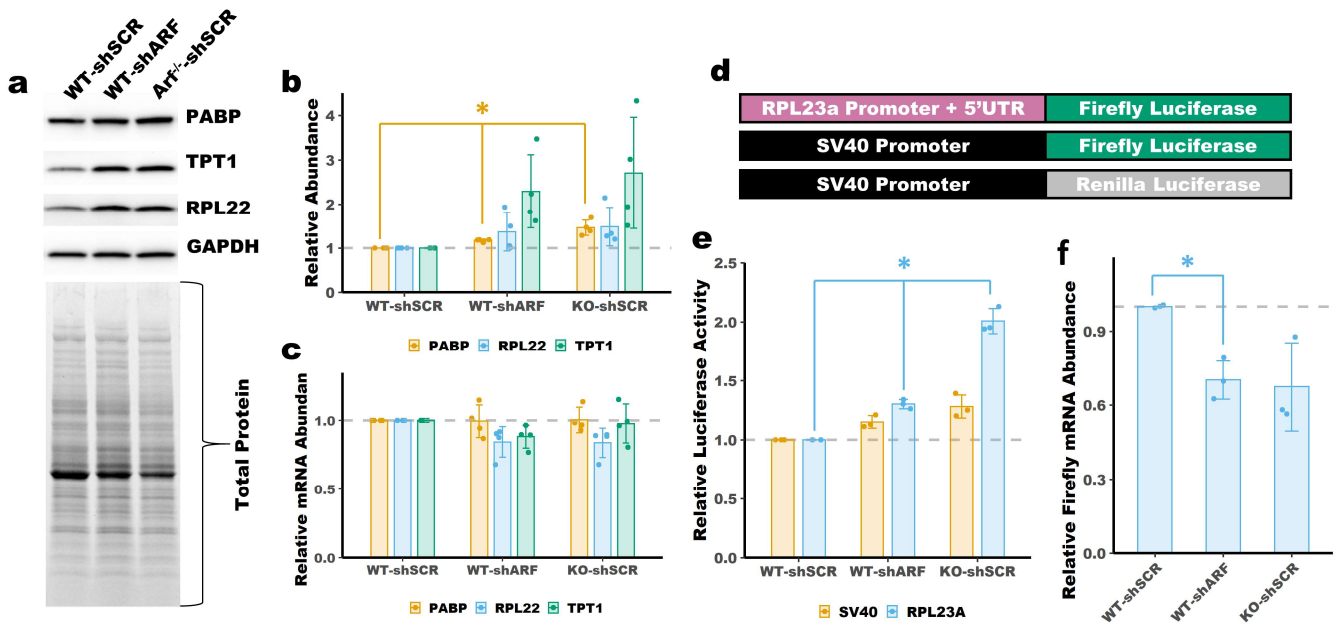

Figure 3: Upregulation of 5'-TOP mRNA translation following loss of ARF

a Immunoblot analysis showing increased protein abundance of PABP, TPT1 and RPL22. **b** Quantitation of blots in panel **a**. Total protein was used for normalization. Mean±SD, n=4. **c** qPCR shows no change in mRNA expression of 5'-TOP mRNAs. Mean±SD, n=4. **d** Schematic of the luciferase reporters used in panels **e** and **f. e** Luciferase activity of a 5'-TOP reporter is increased in ARF-null MEFs. Luciferase activity was normalized to *Renilla* luciferase transfection control and set relative to WT-shSCR. Mean±SD, n=3. **f** qPCR shows no increase e in mRNA expression of the RPL23a reporter. Normalized to *Renilla* luciferase transfection control. Mean±SD, n=3. * *p*-value < 0.05; t-test with Bonferoni correction.

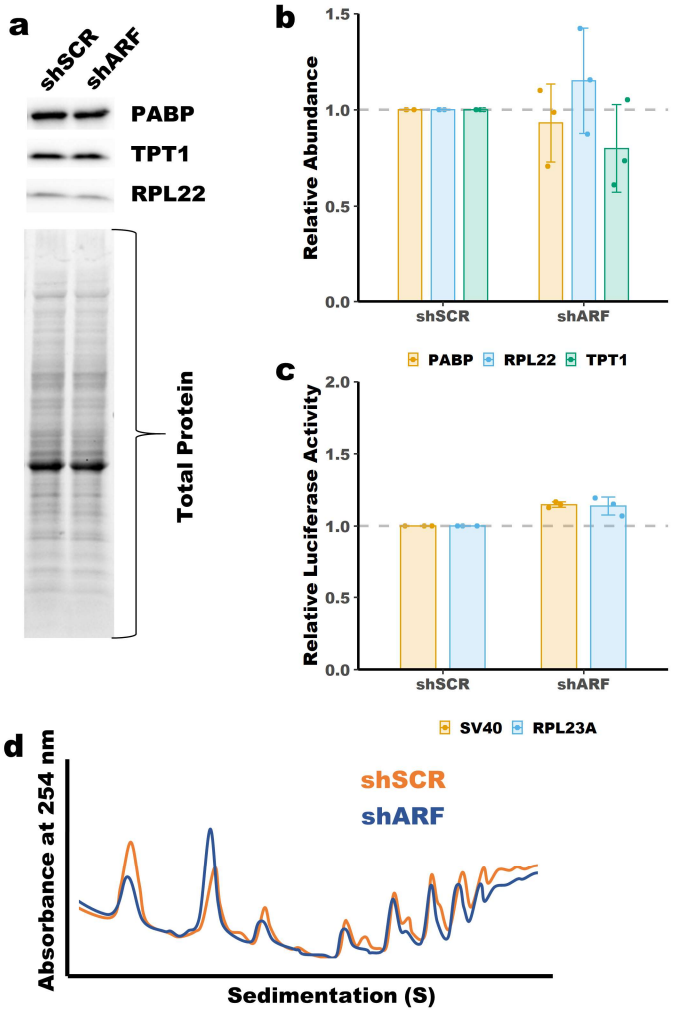

402

403 **Figure 4: 5'-TOP expression is unaffected by ARF knockdown in p53$^{-/-}$ MEFs**

404 **a** Immunoblot analysis showing no change in protein abundance of PABP, TPT1 and RPL22 following ARF
405 knockdown in *p53*$^{-/-}$ MEFs. **b** Quantitation of blots in panel **a**. Total protein was used for normalization.
406 Mean±SD, n=3. **c** No change in luciferase activity of a 5'-TOP reporter following ARF knockdown in *p53*$^{-/-}$ MEFs.
407 Luciferase activity was normalized to *Renilla* luciferase transfection control and set relative to shSCR.
408 Mean±SD, n=3. **d** Polysome profiling showing no change in polysome peaks in *p53*$^{-/-}$ MEFs following
409 knockdown of ARF.

410

411

412

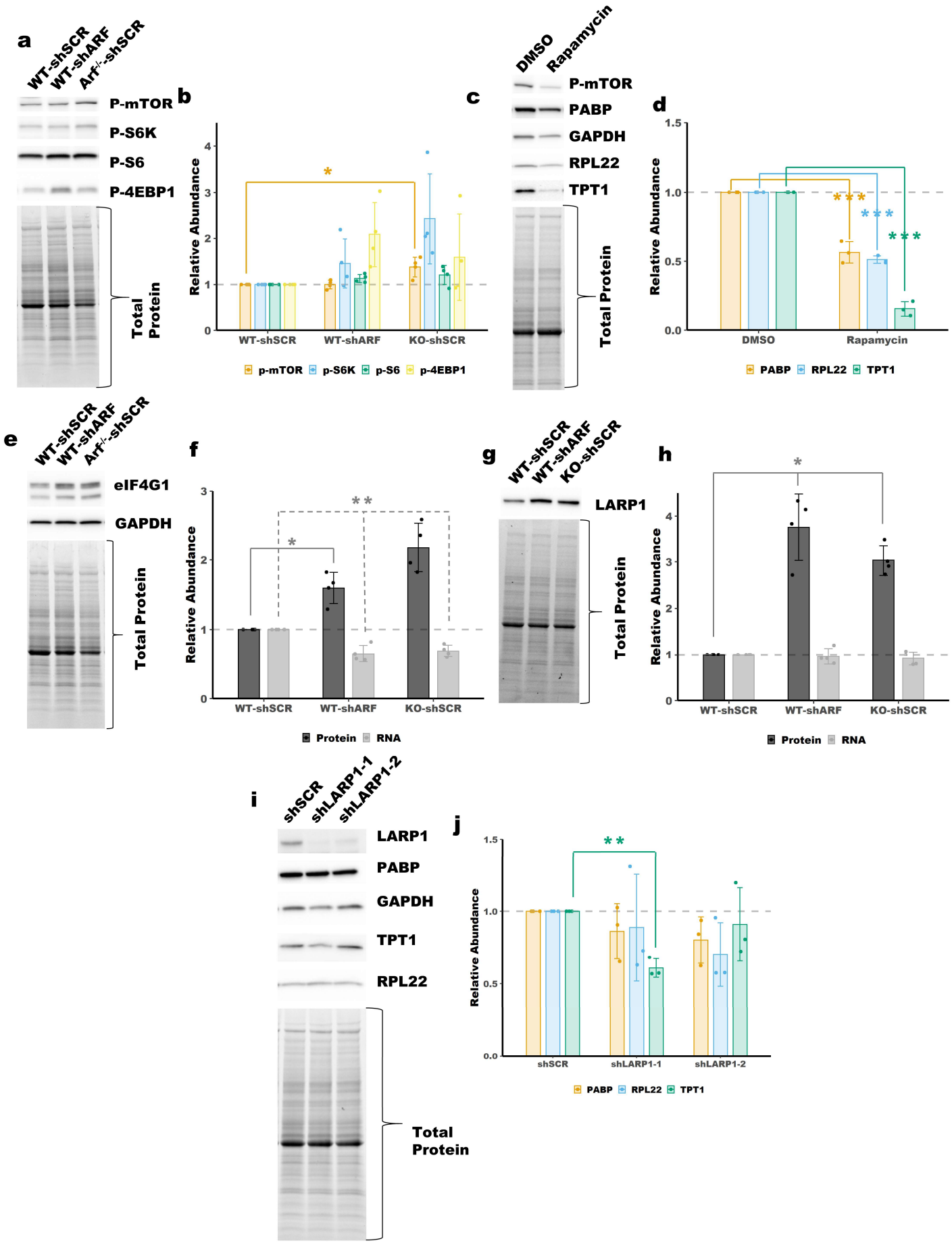
a
WT-shSCR
WT-shARF
Arf-/--shSCR
P-mTOR
P-S6K
P-S6
P-4EBP1
Total Protein
b
Relative Abundance
WT-shSCR
WT-shARF
KO-shSCR
p-mTOR
p-S6K
p-S6
p-4EBP1
c
DMSO
Rapamycin
P-mTOR
PABP
GAPDH
RPL22
TPT1
Total Protein
d
Relative Abundance
DMSO
Rapamycin
PABP
RPL22
TPT1
e
WT-shSCR
WT-shARF
Arf-/--shSCR
eIF4G1
GAPDH
Total Protein
f
Relative Abundance
WT-shSCR
WT-shARF
KO-shSCR
Protein
RNA
g
WT-shSCR
WT-shARF
KO-shSCR
LARP1
Total Protein
h
Relative Abundance
WT-shSCR
WT-shARF
KO-shSCR
Protein
RNA
i
shSCR
shLARP1-1
shLARP1-2
LARP1
PABP
GAPDH
TPT1
RPL22
Total Protein
j
Relative Abundance
shSCR
shLARP1-1
shLARP1-2
PABP
RPL22
TPT1

413

414 **Figure 5: The expression and activity of 5'-TOP mRNA regulators following loss of tumor suppressors**

415 **a** Immunoblot analysis showing activity of mTORC1 in WT and ARF-null MEFs and quantified in **b**. p-mTOR = p-
416 S2484, p-S6K = p-T389 (p70), p-S6 = p-S240/S244, p-4EBP1 = p-T37/T46. Total protein was used for
417 normalization. Mean±SD, n=4 **c** Immunoblot analysis showing expression of 5'-TOP mRNA encoded proteins
418 following treatment with rapamycin (Selleck Chemicals) and quantified in **d.** *Arf*$^{-/-}$ MEFs were treated with 5
419 nM rapamycin for 4 days. Total protein was used for normalization. Mean±SD, n=3. **e** Immunoblot analysis
420 showing increased expression of eIF4G1 in ARF-null MEFs. **f** Quantitation of blot in **e** and qPCR for eIF4G1,
421 total protein was used for normalization of immunoblot, Mean±SD, n=4. **g** Immunoblot analysis showing
422 increased expression of LARP1 in ARF-null MEFs. **h** Quantitation of blot in **g** and qPCR for LARP1, total protein
423 was used for normalization of immunoblot, Mean±SD, n=4. **i** Immunoblot of *Arf*$^{-/-}$ MEFs following knockdown
424 of LARP1 with two different shRNAs. **j** Quantitiation of blot in **i,** total protein was used for normalization of
425 immunoblot, Mean±SD, n=3. *, **, *** *p*-value < 0.05, <0.01, <0.001; t-test with Bonferoni correction.

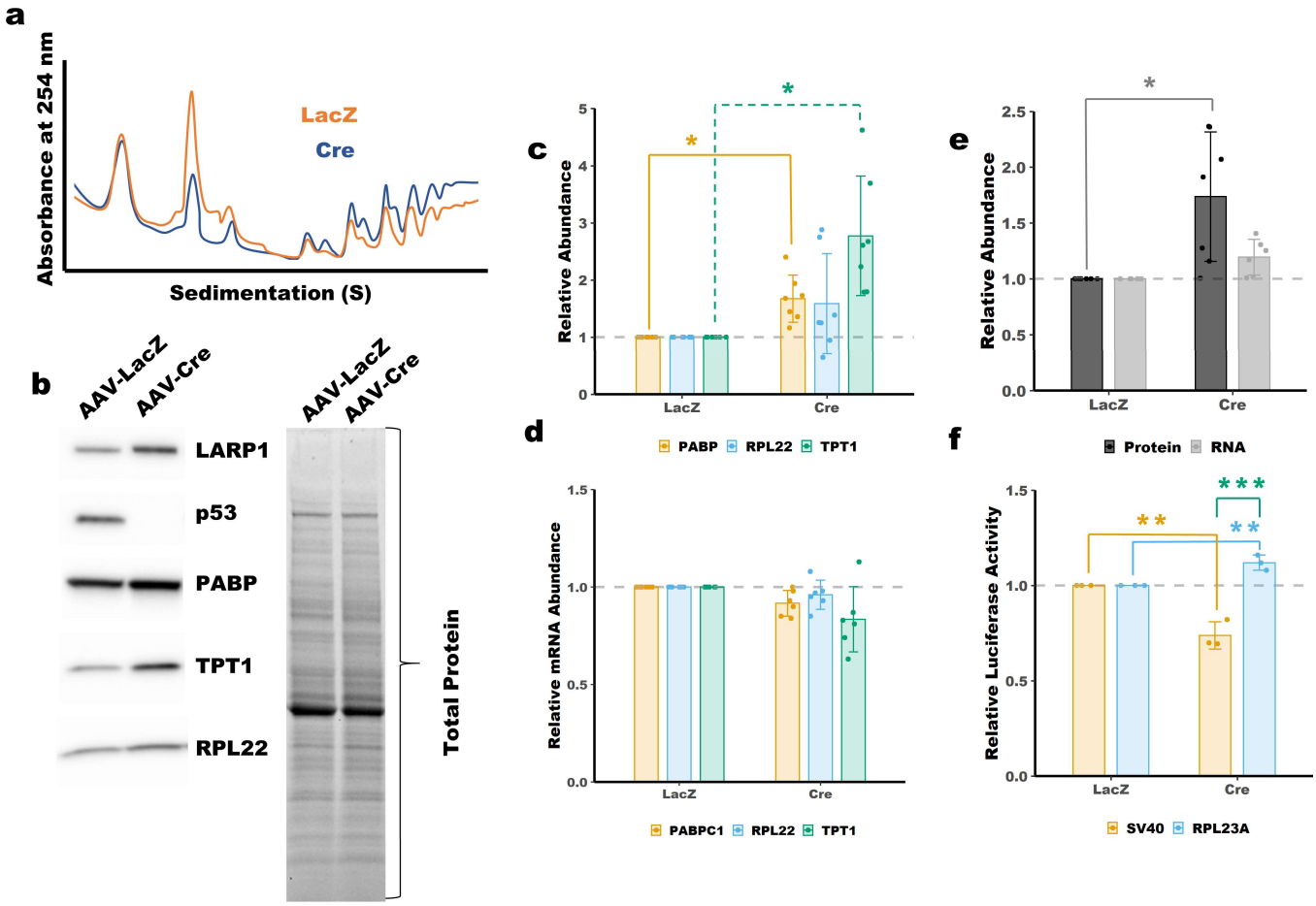

Figure 6: Upregulation of 5'-TOP mRNAs in *p53*$^{-/-}$ MEFs

a Polysome profiling showing increased polysome peaks following knockout of *p53* (Cre). Immunoblot analysis showing increased protein abundance of LARP1, PABP, TPT1 and RPL22 following knockout of *p53* (AAV-Cre). **c** Quantitation of blots in panel **b**. Total protein was used for normalization. Mean±SD, n=7. **d** qPCR shows no change in mRNA expression of 5'-TOP mRNAs following knockout of *p53*. Mean±SD, n=6. **e** Quantitation of blot in **b** and qPCR for LARP1. Mean±SD, n=7(protein), 6(RNA). **f** Luciferase activity of a 5'-TOP reporter is increased in *p53*$^{-/-}$ MEFs. Luciferase activity was normalized to *Renilla* luciferase transfection control and set relative to LacZ control. Mean±SD, n=3. *, **, *** *p*-value < 0.05, <0.01, <0.001; t-test with Bonferoni correction.